Received Sept.11 2020

Accepted Nov.04 2020

Article Type: Research Article

Edited by: Suomeng Dong, Nanjing Agricultural University, China

Running Title: NbPPI1 triggers plant immune responses

The novel peptide NbPPI1 identified from *Nicotiana benthamiana* triggers immune responses and enhances resistance against *Phytophthora* pathogens

Qujiang Wen[1], Manli Sun[1], Xianglan Kong[2], Yang Yang[2], Qiang Zhang[1], Guiyan Huang[3], Wenqin Lu[1], Wanyue Li[2], Yuling Meng[2], Weixing Shan[2]*

1 State Key Laboratory of Crop Stress Biology for Arid Areas and College of Plant Protection, Northwest A&F University, Yangling 712100, China

2 State Key Laboratory of Crop Stress Biology for Arid Areas and College of Agronomy, Northwest A&F University, Yangling 712100, China

3 State Key Laboratory of Crop Stress Biology for Arid Areas and College of life sciences, Northwest A&F University, Yangling 712100, China

* Correspondence: Weixing Shan (wxshan@nwafu.edu.cn)

This article has been accepted for publication and undergone full peer review but has not been through the copyediting, typesetting, pagination and proofreading process, which may lead to differences between this version and the Version of Record. Please cite this article as doi: 10.1111/jipb.13033.

Abstract

In plants, recognition of small secreted peptides, such as damage/danger-associated molecular patterns (DAMPs), regulates diverse processes, including stress and immune responses. Here, we identified an SGPS (Ser-Gly-Pro-Ser) motif-containing peptide, *Nicotiana tabacum* NtPROPPI, and its two homologs in *Nicotiana benthamiana*, NbPROPPI1 and NbPROPPI2. *Phytophthora parasitica* infection and salicylic acid (SA) treatment induced *NbPROPPI1/2* expression. Moreover, SignalP predicted that the 89-amino acid NtPROPPI includes a 24-amino acid N-terminal signal peptide and NbPROPPI1/2-GFP fusion proteins were mainly localized to the periplasm. Transient expression of *NbPROPPI1/2* inhibited *P. parasitica* colonization, and *NbPROPPI1/2* knockdown rendered plants more susceptible to *P. parasitica*. An eight-amino-acid segment in the NbPROPPI1 C-terminus was essential for its immune function and a synthetic 20-residue peptide, NbPPI1, derived from the C-terminus of NbPROPPI1 provoked significant immune responses in *N. benthamiana*. These responses led to enhanced accumulation of reactive oxygen species, activation of mitogen-activated protein kinases, and up-regulation of the defense genes *Flg22-induced receptor-like kinase* (*FRK*) and *WRKY DNA-binding protein 33* (*WRKY33*). The NbPPI1-induced defense responses require *Brassinosteroid insensitive 1-associated receptor kinase 1* (*BAK1*). These results suggest that NbPPI1 functions as a DAMP in *N. benthamiana*; this novel DAMP provides a potentially useful target for improving resistance to *P. parasitica*.

Keywords: DAMP, Disease resistance, *Phytophthora parasitica*, SGPS peptides, Tobacco

INTRODUCTION

Peptide ligands are small endogenous signals that orchestrate plant development and immune signaling (Tavormina et al. 2015; Olsson et al. 2019; Segonzac and Monaghan 2019). Many of these ligands function as damage/danger-associated molecular patterns (DAMPs) (Boller and Felix 2009; Heil et al. 2012; Wu and Zhou 2013). In contrast to pathogen-associated molecular patterns (PAMPs), which are derived from invading microbes, DAMPs are host-derived molecules that are passively released upon host damage or actively processed and released upon tissue damage or other stimuli. DAMPs activate immune responses to defend against infection or facilitate repair of damaged tissue (Heil and Land 2014; Gust et al. 2017; De Lorenzo et al. 2018). DAMPs and other peptide ligands are recognized by a large family of pattern-recognition receptors (PRRs) (Zipfel 2014). Upon binding of the DAMP peptide ligand to its cognate PRR, the plant initiates robust immune responses involving up-regulation of defense genes, production of reactive oxygen species (ROS), and deposition of callose (Asai et al. 2002; Chinchilla et al. 2007; Denoux et al. 2008; Mueller et al. 2012).

Multiple DAMP peptides have been identified from *Arabidopsis thaliana*. For example, PLANT ELICITOR PEPTIDE 1 (PEP1) is a 23-amino-acid peptide derived from *PRECURSOR OF PEPTIDE 1* (*PROPEP1*) (Huffaker et al. 2006). Upon recognition by PEP RECEPTOR 1 and 2 (PEPR1/2), the plant initiates a wound-associated immune response to defend against hemibiotrophic bacteria and necrotrophic fungi (Krol et al. 2010; Tavormina et al. 2015). PAMP-INDUCED SECRETED PEPTIDE 1 and 2 (PIP1/2), which are generated through C-terminal cleavage of PrePIP1/PrePIP2, bind to RECEPTOR-LIKE KINASE 7 (RLK7) to provoke an immune response in *A. thaliana* that is then amplified through FLAGELLIN-SENSING 2 (FLS2) signaling (Hou et al. 2014). A targeted *in silico*

approach identified the precursor of SERINE-RICH ENDOGENOUS PEPTIDE 12 (PROSCOOP12) in *A. thaliana*; its putative mature form, the peptide SCOOP12, enhanced resistance to the bacterial pathogen *Erwinia amylovora* in a *BRASSINOSTEROID INSENSITIVE 1-ASSOCIATED RECEPTOR KINASE 1* (*BAK1*)-dependent manner (Gully et al. 2019).

SGPS (Ser-Gly-Pro-Ser) motif-containing peptides (SGPS peptides) are characterized by conserved Ser, Gly/Ala/Val, Pro, and Ser residues at the C-terminal and an N-terminal signal peptide (Vie et al. 2015; Hou et al. 2019). SGPS peptides include CLAVATA3 (CLV3)/ENDOSPERM SURROUNDING REGION (ESR)-related (CLE) peptides (Oelkers et al. 2008; Kaeothip et al. 2013), INFLORESCENCE DEFICIENT IN ABSCISSION (IDA)-like members (IDLs) (Vie et al. 2015), PIPs and PIP-LIKE (PIPL) peptides (Hou et al. 2014), C-TERMINALLY ENCODED PEPTIDE 1 (CEP1) (Ohyama et al. 2008), and PEP1 (Huffaker et al. 2006), which are all found in *A. thaliana*. Although there are significant sequence similarities among different SGPS peptides, they serve diverse roles in immune signaling. PIP1 and PIP2 are induced by PAMPs, and enhance immune responses and pathogen resistance in *A. thaliana* (Hou et al. 2014). Induction of *IDL6* caused by *Pseudomonas syringae* infection facilitated pathogen invasion by increasing expression of the polygalacturonase (PG) gene *ADPG2* and PG activity in *A. thaliana* leaves, contributing to cell wall disruption (Wang et al. 2017). Overexpression of *PIP3* impaired the flagellin 22 peptide (flg22)-induced immune response and rendered plants more susceptible to *Botrytis cinerea* and *P. syringae*. It is possible that this occurs through negative feedback on the expression of PAMP-induced genes, like *PIP1* and *PIP3*, via the transcription factors WRKY DNA-BINDING PROTEIN 18 (WRKY18), WRKY33, and WRKY40 (Najafi et al. 2020).

Peptide ligands are recognized by the PRRs leucine-rich repeat receptor kinases (LRR-RKs) on the plasma membrane (Shiu and Bleecker 2001; Wang et al. 2020). Following ligand binding, LRR-RKs form dynamic complexes with regulatory co-receptor kinases to activate immune signaling (Perraki et al. 2018). The best characterized co-receptor is BAK1, a member of the somatic embryo receptor kinase (SERK) family (Chinchilla et al. 2007；Heese et al. 2007). BAK1 participates in PEP1 binding to PEPR1/2 (Huffaker et al. 2006; Huffaker et al. 2011; Hander et al. 2019), Phytosulfokine (PSK) recognition by PSK RECEPTOR 1/2 (PSKR1/2) (Matsubayashi and Sakagami 1996; Mosher et al. 2013; Sauter 2015; Zhang et al. 2018), PIP1/2 binding to RLK7, and SCOOP12 binding (Chen et al. 2020). Multiple ligand-induced signaling pathways converge at BAK1, facilitating simultaneous and integrated control of the immune responses in plants (Chinchilla et al. 2007; Postel et al. 2010; Schulze et al. 2010). Different peptide ligands that depend on BAK1-mediated signaling, like PEP1 (Huffaker et al. 2006) and PIP1 (Hou et al. 2014), are likely to work synergistically to induce immune signaling. Additionally, antagonistic effects might occur when the binding of specific ligands has a negative effect on the formation of BAK1-associated receptor complexes (Chen et al. 2020). For example, RAPID ALKALINIZATION FACTOR23 (RALF23) inhibits the immune response activated by receptor kinase FLS2-EF-Tu receptor (EFR) signaling. Upon ligand recognition, FLS2 and EFR form dynamic complexes with their co-receptor BAK1 via the scaffolding protein FERONIA (FER). FER is the receptor for RALF23, and the interaction between RALF23 and FER reduces ligand-induced FLS2/EFR-BAK1 complex formation, and therefore inhibits the pattern-triggered immunity (PTI) response (Li et al. 2002; Matos et al. 2008; Srivastava et al. 2009; Sun et al. 2011; Stegmann et al. 2017).

In this study, we sought to identify a recognition-based disease resistance strategy for broad-spectrum, durable disease resistance in crops. We employed *Nicotiana tabacum* to identify potential endogenous peptide ligands that activate immune responses against pathogens. We identified such a peptide ligand, NtPROPPI in *N. tabacum* and its homologs, NbPROPPI1/2, in *Nicotiana benthamiana*. We show that NbPROPPI1 was a novel DAMP capable of initiating immune responses and promoting disease resistance in *N. benthamiana* against the oomycete pathogen *Phytophthora parasitica* and *Phytophthora infestans*. The *NbPROPPI1*-mediated immune responses involve enhanced accumulation of ROS, activation of mitogen-activated protein kinases (MAPKs) and up-regulation of the defense genes *Flg22-induced receptor-like kinase* (*FRK*) and *WRKY DNA-binding protein 33* (*WRKY33*). The identified novel endogenous DAMP derived from *N. benthamiana* could provide a useful gene for breeding for disease resistance against *P. parasitica.*

RESULTS

Identification of *PROPPI*

To screen for genes that are involved in the plant-pathogen interactions and stimulate immune responses in plants, we constructed a cDNA library using Gateway technology with tissue from *N. tabacum* leaves infected with *P. parasitica*. Using high-throughput *Agrobacterium tumefaciens*-mediated transient expression in leaves of *N. tabacum* cultivar HD, we identified a novel protein-coding gene, *NtPROPPI*, which induced weak chlorosis on *N. tabacum* cultivars YunYan85, QinYan95, and HD, but not on *N. tabacum* cultivar K346, *N. benthamiana*, potato (*Solanum tuberosum*) (differential line R5), or tomato (*Solanum lycopersicum*) cultivar Alisa Craig (Figure S1A).

NtPROPPI encodes a predicted peptide of 89 amino acid residues and includes a 24-amino acid N-terminal signal peptide, as predicted by the SignalP 5.0 server (http://www.cbs.dtu.dk/services/SignalP). BLAST analysis of the NtPROPPI protein sequence showed that it belongs to a family of SGPS (Ser-Gly-Pro-Ser) - GxGH (Gly-X-Gly-His) motif-containing peptides and shares a conserved C-terminal sequence with IDA/IDLs (Vie et al. 2015) and AtPIPs (Hou et al. 2014). The SGPS motif also exists in potato and tomato plants (Figure S2). To identify putative homologs in *N. benthamiana*, the full-length protein sequence of NtPROPPI was used as a query for BLAST analysis on the Sol Genomics Network (https://solgenomics.net/). Five predicted proteins in *N. benthamiana* with an SGPS motif were identified as NtPROPPI homologs, and two of the homologs were named as NbPROPPI1 (Niben101Scf00803g01016.1, 95.6% sequence similarity) and NbPROPPI2 (Niben101Scf03747g00005.1, 91.2% sequence similarity) due to their high protein sequence similarities to NtPROPPI (Figure 1A).

The localization of proteins is often related to their function. To investigate the sub-cellular localization of NbPROPPI1 and NbPROPPI2, green fluorescent protein (GFP) was fused to the C-terminus of NbPROPPI1 and NbPROPPI2, as the N-terminus is predicted to be removed in processing to the mature form. The fusion constructs were driven by the *Cauliflower mosaic virus* 35S (CaMV 35S) promoter and transiently expressed in *N. benthamiana* leaves using agroinfiltration. The NbPROPPI-GFP fusion protein was monitored by confocal microscopy. Our imaging analysis revealed that NbPROPPI1-GFP (Figure 1B) and NbPROPPI2-GFP (Figure 1C) were distributed in the periplasm after plasmolysis, as shown by the fluorescent signal, indicating that NbPROPPI1 and NbPROPPI2 may be secreted proteins, which is consistent with the SignalP 5.0 analysis.

We further tested whether *NbPROPPI1* and *NbPROPPI2* could trigger cell death in *N. tabacum* by using a transient expression assay. *NbPROPPI1* and *NbPROPPI2* induced chlorosis on three *N. tabacum* cultivars, YunYan85, QinYan95, and HD, but not on *N. tabacum* cultivar K346, *N. benthamiana*, potato (differential line R5), or tomato cultivar Alisa Craig (Figure 2A). To confirm the potential role of *NbPROPPI* in triggering immune responses, *N. tabacum* cultivar HD leaves were infiltrated with *A. tumefaciens* GV3101 cells carrying *NbPROPPI1* or *β-glucuronidase* (*GUS*) constructs (as a control), followed by infection with *P. parasitica*. Over-expressing *NbPROPPI1* significantly enhanced resistance of *N. tabacum* cultivar HD to *P. parasitica* (Figure 2B), as indicated by smaller lesions compared to the control (Figure 2C). Consistent with larger lesion size, *P. parasitica* biomass was more abundant in *GUS*-expressing control lines than in the *NbPROPPI1*-expressing lines (Figure 2D). The similar results were obtained for *NtPROPPI* (Figure S2B-D). These results indicated that *NbPROPPI1* enhances *N. tabacum* resistance against *P. parasitica* infection when over-expressed *in planta*, and thus functions as a positive immune regulator against *P. parasitica*.

NbPROPPI expression is induced by pathogen treatment and SA treatment

To examine whether the expression of *NbPROPPI* is responsive to *P. parasitica* infection, we employed quantitative real-time PCR (qRT-PCR) to measure *NbPROPPI1/2* transcript levels in the *P. parasitica*-inoculated wild-type *N. benthamiana* leaves at different time points. The expression of *NbPROPPI1* and *NbPROPPI2* remained at relatively low levels under normal conditions but peaked at 24 h post inoculation and then later declined (Figure 3A). These results indicated that *NbPROPPI1/2* were responsive to *P. parasitica* at the early stage of infection.

Since defense-related genes are commonly provoked by various signals or hormones (Gust et al. 2017) and some DAMPs were induced by mechanical wounding (Chen et al. 2020), we analyzed the influence of hormones and wounding on *NbPROPPI1*/*2* expression. The *NbPROPPI1* and *NbPROPPI2* transcripts were induced by methyl salicylate (MeSA) (Figure 3B), but not by the ethylene precursor 1-aminocyclopropane-1-carboxylate (ACC) (Figure 3C), methyl jasmonate (MeJA) (Figure 3D), or by wounding (Figure S3).

NbPPI treatment enhances plant resistance against *Phytophthora* pathogens

Given that NbPROPPI contains an SGPS motif, which is also found in PIPs and IDA proteins that are known to regulate plant immunity (Hou et al. 2014; Vie et al. 2015), we hypothesized that the putative mature form of NbPROPPI, NbPPI, plays a role in plant immunity. To confirm this, we synthesized the putative mature NbPPI1 and NbPPI2 peptides deduced from the conserved C-terminal sequence encoded by *NbPROPPI1* and *NbPROPPI2* (Table S2).

We introduced 1 μM NbPPI1 and NbPPI2 into *N. benthamiana* leaves. After 24 hours of treatment, the detached leaves were challenged with *P. parasitica* or *P. infestans*. Treatment with 1 μM NbPPI1 or NbPPI2 enhanced the resistance of *N. benthamiana* against both *P. parasitica* and *P. infestans*, as indicated by the reduced lesion size in leaves treated with NbPPI1 and NbPPI2 compared to the control plants. In addition, quantitation of *P. parasitica* and *P. infestans* biomass consistently revealed limited colonization (Figure 4) in NbPPI1- and NbPPI2-infiltrated plants, indicating that NbPPI1 and NbPPI2 play positive roles in defending against *Phytophthora* pathogens.

NbPPI activates plant immune responses

Given that *NbPROPPI* expression is quickly induced by *P. parasitica* invasion, with its encoded peptide secreted to the periplasm space, and that NbPPI1/2 significantly enhanced resistance against *P. parasitica*, we inferred that *NbPROPPI* might encode a DAMP peptide. Treatment of *N. benthamiana* leaves with NbPPI1 resulted in a moderate but significant up-regulation of the transcription factor genes *WRKY33* (Figure 5A) and *FRK* (Figure 5B) compared with the control. However, this up-regulation of *WRKY33* and *FRK* were weaker than that induced by flg22. Next, we detected the MAPK signaling activation (Asai et al. 2002; Galletti et al. 2011; Cederholm and Benfey 2015) upon NbPPI1 treatment using western blotting. The results showed that NbPPI1 strongly activated MPK6 and slightly activated MPK3 in *N. benthamiana* (Figure 5C).

ROS production functions as an important signal in multiple biological processes, including biotic and abiotic stresses, and plant development (Wang et al. 2020). Compared with flg22 treatment alone, treatment with both NbPPI1 and flg22 simultaneously had an additive effect on ROS production (Figure 5D). Meanwhile, treatment with NbPPI1 and flg22 simultaneously triggered more abundant callose deposition than flg22 alone, though NbPPI1 induced weaker callose accumulation than flg22. Furthermore, silencing of *NbPROPPI* by virus-induced gene silencing (VIGS) assay impaired flg22-induced callose deposition compared to the control (Figure 5E, 5F). In conclusion, NbPPI1 functions as a novel DAMP in *N. benthamiana*, and is involved in enhanced resistance against *P. parasitica.*

NbPROPPI silencing reduces plant resistance to *P. parasitica*

To confirm the role of *NbPROPPI* in plant immunity, we performed gene silencing assays in *N. benthamiana*. Because the sequences of *NbPROPPI1* and *NbPROPPI2* share a high level of similarity (94.57%) and possible functional redundancy (Figure 4), both genes were silenced by the VIGS assay. The transcript levels of the *NbPROPPI* genes were reduced by 70-80% in the plants harboring the *TRV2-NbPROPPI* construct compared to the *TRV2-GFP* control plants (Figure 6D). When challenged with *P. parasitica*, the infection lesions on *NbPROPPI*-silenced plants were more severe than on the control plants (Figure 6A, 6B). In addition, quantitation of *P. parasitica* biomass (Figure 6C) revealed that *NbPROPPI*-silenced plants showed enhanced disease susceptibility to *P. parasitica*. These findings suggest that *NbPROPPI* is a positive immune regulator in *N. benthamiana* against *P. parasitica*.

A C-terminal region outside of the SGPS motif in NbPPI1 is essential for its immune function

Sequence alignment identified a conserved C-terminal region consisting of 8 amino acid residues that was present in NtPROPPI, NbPROPPI1, and NbPROPPI2 but was absent from AtPIPs (Figure S2). To examine whether the conserved C-terminus of the SGPS peptide NbPPI1 is required for its immune function, we synthesized a truncated NbPPI1 peptide that contained a deletion of the 8 C-terminal amino acid residues (NbPPI1-ΔC8) and analyzed its immune activity. *N. benthamiana* leaves were infiltrated with 1 μM NbPPI1 or 1 μM NbPPI1-ΔC8, and followed by inoculation with *P. parasitica* after 24 hours. Two days after *P. parasitica* infection, the plants treated with NbPPI1 showed significantly smaller lesions compared to the control plants. The lesion sizes in leaves treated with NbPPI1-ΔC8 were much larger than those of leaves treated

with NbPPI1 and the growth of *P. parasitica* was significantly restricted in NbPPI1-treated plants compared to the NbPPI1-ΔC8-treated plants (Figure 7A). The seedlings treated with NbPPI1 exhibited much shorter roots compared to the seedlings treated with H_2O (as a control). Root growth of seedlings treated with NbPPI1-ΔC8 was similar to the control, and was significantly different from those treated with NbPPI1 (Figure 7B). Our results resemble the growth inhibition effect of DAMPs or PAMPs, such as PEP1 (Huffaker et al. 2006) and PIP1 (Hou et al. 2014) on seedlings. Furthermore, the synergistic effect of NbPPI1 and flg22 on ROS production was abolished by the deletion of the 8 C-terminal amino acid residues of NbPPI1 (Figure 7C). Taken together, these results showed that the C-terminal region outside of the SGPS motif plays essential roles in the NbPPI1-mediated immune response and DAMP function.

The NbPPI1-mediated defense response requires *BAK1*

In many cases, the corresponding receptor for DAMP recognition requires BAK1 for full activation (Chinchilla et al. 2007; Heese et al. 2007), as is the case for Pep1, PSK, PIP1/2, and SCOOP12 (Chen et al. 2020). To explore whether NbPPI1-induced immune signaling is *BAK1*-dependent, we generated *BAK1*-silenced plants using VIGS assay and examined NbPPI1-induced immune responses and disease resistance in *BAK1*-silenced plants. The transcript levels of *NbBAK1* were reduced by 85% in the plants harboring the *TRV2-BAK1* construct compared to the *TRV2-GFP* control plants (Figure 8D). About 21 days post-agroinfiltration with VIGS constructs, *P. parasitica* was inoculated on detached leaves. Induction of *NbPROPPI1* expression was not affected in *BAK1*-silenced and *TRV2-GFP* control plants upon inoculated with *P. parasitica* (Figure S4). However, NbPPI1-mediated resistance to *P. parasitica* was hindered in the *BAK1*-silenced plants. Quantitation of *P. parasitica* biomass revealed that

the *BAK1*-silenced plants showed enhanced disease susceptibility to *P. parasitica* (Figure 8A). Flg22-induced ROS production was significantly decreased in *BAK1*-silenced plants, and the synergistic effect of NbPPI1 on flg22-induced ROS production was almost completely abolished (Figure 8B). Furthermore, NbPPI1-triggered up-regulation of *WRK33* was largely abolished in *BAK1*-silenced plants (Figure 8C). These results suggested that NbPPI1- and flg22-induced signaling and their integration are partially dependent on *BAK1*.

DISCUSSION

Plant peptides secreted as signal transmitters for cell-to-cell communication are indispensable for plant growth and development, and defense processes in plant-microbe interactions (Hu et al. 2018). To develop a recognition-based disease resistance strategy for broad-spectrum, durable disease resistance in crops, we screened for endogenous peptide ligands that activate immune responses against pathogens in *N. tabacum* by employing an *A. tumefaciens*-mediated transient expression method. After testing on the leaves of *N. tabacum*, numerous candidates were found, including the small protein NtPROPPI with a predicted signal peptide.

Overexpression of *NtPROPPI1*, *NbPROPPI1*, or *NbPROPPI2* in *N. tabacum* leaves led to weak cell death and enhanced resistance against *P. parasitica* (Figure 2, S1). Cell death is at the center of immune responses, and is often caused by pathogen recognition via NB-LRRs in plants (Coll et al. 2011). However, DAMP-induced cell death has rarely been reported in plants. A non-specific cell death phenotype was considered to be the consequence of a putative DAMP released by family 17 glycosyl hydrolases of the tomato pathogen *Cladosporium fulvum* (CfGH17) (Ökmen et al. 2019). Oligogalacturonides (OGs) are released as an immune signal in relatively low amounts, as hyper-accumulation of OGs was

shown to elicit tissue necrosis due to an overactive immune response (Cervone et al. 1987; Benedetti et al. 2018). The signaling pathway under DAMP-induced cell death is still elusive. In our study, cultivar-specific weak cell death induced by *NtPROPPI* and *NbPROPPI1/2* was largely resulted from their different genetic backgrounds. We inferred that variation of PPI receptors, such as their immune activities or expression levels, or downstream factors in different cultivars may contribute to the cultivar-specific response. RLK7 was identified as the receptor for PIP1 (Hou et al. 2014), which is a homolog of *NbPROPPI* in *A. thaliana*. Homologs of RLK7 in *N. benthamiana* and *N. tabacum* cultivars YunYan85, QinYan95, and HD could be examined for potential differential ligand recognition. Additionally, further studies should focus on the receptors for PPI in *N. benthamiana* and *N. tabacum*.

Plant genomes encode numerous small secreted peptides, which have recently emerged as key signaling molecules of stress responses in plants (Ghorbani et al. 2015). Most peptides are synthesized as preproproteins and processed by successive proteolytic cleavages through the secretory pathway (Matsubayashi 2011). Conserved sequence motifs enable their specific ligand-receptor recognition and thus are vital for their signaling function. NbPROPPI1/2 belong to a family of SGPS - GxGH motif-containing peptides and share a conserved C-terminal SGPS-GxGH motif with AtPIPs (Hou et al. 2014). Through sequence alignment of NbPROPPI1/2 homologs in *A. thaliana* and solanaceous crops, an additional distinct region of 8 amino acid residues in their C-termini was identified in Solanaceae (Figure S2). Deletion of the 8 amino acid residues disrupted the immune function of NbPPI1, suggesting that the 8 amino acid residues are indispensable for receptor recognition for NbPPI1 homologues in solanaceous crops.

Transcriptomic analysis of *N. benthamiana* roots infected by the hemibiotrophic pathogen *Phytophthora palmivora* revealed that a PIP homolog Tip Induced Plant Transcript switched On by *P. palmivora* (TOPTIP)-encoding gene, namely *NbPROPPI2* in our study, was specifically induced in the root tip after *P. palmivora* infection (Evangelisti et al. 2017). In our study, *NbPROPPI1/2* could be induced by *P. parasitica* infection and SA treatment (Figure 3). In addition, treatment with NbPPI1 activated SA signaling, as evidenced by up-regulation of the SA-inducible gene *PATHOGENESIS RELATED1* (*PR1*) (Figure S5). Thus, *NbPROPPI1* expression and SA signaling form a positive feedback loop.

Since SA is a signaling molecule in the systemic acquired resistance pathway (Sandhu et al. 2009) and plays a central role in plant disease resistance (Choi et al. 2016), it is possible that NbPPI1 would induce systemic resistance if it was able to provoke a secondary signal amplification. This is the case with the first known peptide hormone systemin, an 18-residue peptide (Pearce et al. 1991), which mediates the systemic resistance that occurs in wounding response by orchestrating various defense signaling pathways in tomato. Upon mechanical wounding, systemin derived from PROSYSTEMIN induces the production of PROTEASE INHIBITOR I and II (PI-I and PI-II) and activates the local biosynthesis of jasmonic acid (JA) and jasmonoyl isoleucine (JA-Ile), which travel via the vascular tissue into the leaf and induce defense responses at both primary infected sites and distal regions (Li et al. 2002; Sun et al. 2011). PROSYSTEMIN expression is JA-inducible, and systemin and JA amplify wound signaling.

BAK1 is a co-receptor that regulates numerous ligand-binding LRR-RK-induced immune responses, including fig22-FLS2, EF-TU-EFR, and

PEP1-PEPR1 signaling (Chinchilla et al. 2007; Heese et al. 2007; Chaparro-Garcia et al. 2011; Yamada et al. 2016). Although the receptor responsible for detecting NbPPI1 in *N. benthamiana* is unknown, we observed a requirement of *BAK1* in the NbPPI1-induced immune responses. Previous studies revealed that upon interaction with flg22, FLS2 forms a functional complex with BAK1 for signal transduction (Sun et al. 2013). We inferred that BAK1 may serve as a co-receptor of NbPROPPI1. Furthermore, it is also possible that under treatment with NbPPI1 and flg22, the binding of NbPPI1 would enhance the complex formation between FLS2 and BAK1 to facilitate signaling activation. Alternatively, since BAK1 is required for the signaling function of multiple PAMPs and DAMPs, the binding of NbPPI1 could affect other ligand signaling pathways by competitive binding with BAK1.

NbPROPPI1 induces robust basal immune responses, including enhanced ROS accumulation, MAPKs activation, and up-regulation of the defense genes *FRK* and *WRKY33*. Manipulation of host immunity signaling by increasing *NbPROPPI1* expression levels might confer broad-spectrum, durable disease resistance in crops. In conclusion, we have identified a novel DAMP peptide gene, *NbPROPPI1*, from *N. benthamiana* that has a potential to facilitate the development of crops with broad-spectrum disease resistance to pathogens.

MATERIALS AND METHODS

Plant materials and growth conditions

N. benthamiana and *N. tobacum* was grown as previously described (Fan et al. 2018). The *N. benthamiana* and *N. tobacum* seeds were sterilized with 75% ethanol for 1 min and 1% NaClO for 10 mins, and sown on Murashige and Skoog (MS) nutrient medium. After 2 weeks, the seedlings were transferred to a matrix

containing soil and vermiculite (1:2), and grown in a 28°C climate chamber with 14 hours of light per 24 hours for 6 weeks.

Pathogen growth and infection assays

Phytophthora parasitica strain Pp016 and *P. infestans* strain Pi88069 were used for plant infection assays. *P. parasitica* strain 1121 was created from Pp016 and stably expresses endoplasmic reticulum-localized GFP under the control of the constitutive *Hsp70* promoter of *Bremia lactucae*. *P. parasitica* was cultured on 5% (v/v) carrot juice agar medium with 0.01% (w/v) $CaCO_3$ and 0.002% (w/v) β-sitosterol at 23°C.

For pathogenic infection assay in *N. benthamiana* and *N. tobacum*, 5-mm mycelium plugs cut from *P. parasitica* cultures were used to inoculate detached leaves. Lesion diameters were measured at 2 days post-inoculation (dpi). Student's *t*-test was conducted for statistical analysis.*P. infestans* strain Pi88069 was cultured on rye agar medium at 18°C for about 10 days before zoospore production. The hyphae were flooded with 5 mL cold dH_2O, and were scraped to release sporangia (Wang et al. 2015). About 8000 zoospores were used to inoculate detached leaves. Lesion diameters were measured after incubating at 18°C for about 5 days.

Three biological replicates were included with at least 10 leaves per replicate. To quantitate pathogen biomass, qPCR assays were employed using the designed primers listed in Table S1. Leaf discs around the inoculated sites (1 cm in diameter) from the infected leaves were collected as one sample in each plant. Genomic DNA was extracted using the cetyltrimethylammonium bromide (CTAB) method and used as templates in qPCR experiments. The pathogen quantitation was determined by the ratio between pathogen and plant genomic

DNA. Three independent experiments were performed and the statistical significance was determined based on Student's *t*-test.

Plasmid Constructs

For transient expression assays, the fragments of *NtPROPPI*, *NbPROPPI1*, and *NbPROPPI2* were amplified from *N. tabacum* and *N. benthamiana* cDNA using locus-specific primers (Table S1). The products were separately inserted into the GATEWAY vector pMDC32 (Gehl et al. 2009) downstream at *KpnI* and *SpeI* sites to generate *35S:NtPROPPI*, *35S:NbPROPPI1* and *35S:NbPROPPI2*.

To determine subcellular localization, fusion protein constructs *NbPROPPI1-GFP*，*NbPROPPI2-GFP*, and *PM-mCherry* were obtained by overlapping PCR using specific primers (Table S1), and were inserted into vector pMDC32 at *KpnI* and *SpeI* sites.

To generate VIGS constructs, a 120-bp specific fragment of *NbPROPPI*, designed using the SGN VIGS tool (Fernandez-Pozo et al. 2015), was amplified from *N. benthamiana* cDNA and cloned into the binary vector pTRV2 (Liu et al. 2002) at *EcoRI* and *BamHI* sites. *pTRV2:PDS*, *pTRV2:BAK1*, and *pTRV2:GFP* were constructed in the same manner. All constructs were confirmed by sequencing. The primers are listed in Table S1 and were synthesized from Qingke Biological Technology Co., LTD (Xi'an, China).

Construction of cDNA Library

Total RNA from leaves of the *N. tabacum* cultivar HD inoculated with *P. parasitica* at 2 dpi was extracted using TRIzol reagent (Invitrogen, Carlsbad, CA, USA) according to the product manuals. The concentration and purity of the total RNA were determined by spectrophotometry at 260 nm and 280 nm wavelengths

and gel electrophoresis. The total mRNAs were purified from the total RNA by using Oligotex-dT30 (Super) mRNA Purification Kit (Takara, China) according to the manufacturer's instructions. The CaMV 35S promoter sequence and the *attP*-spanning region in the Gateway vector pDONR222 (Invitrogen, Carlsbad, CA, USA) were amplified and inserted into the multiple cloning sites of the *Agrobacterium tumefaciens*-mediated plant expression vector pCAMBIA0380 at *HindIII* site to create the p1104D vector. The cDNAs were cloned into the p1104D vector by Gateway technology (Curtis and Grossniklaus 2003), using CloneMiner cDNA Library Construction Kit (Invitrogen, Carlsbad, CA, USA) according to the manufacturer's instructions.

Synthetic peptides

Peptides with 98% purity level were synthesized by Thermo Science & Technologies Co., LTD (Xi'an, China). Their sequence information is listed in Table S2. The peptides were diluted in water to the final concentration used for the assays and infiltrated into plant leaves using needleless syringes.

Transient expression

A. tumefaciens GV3101 strains carrying the respective constructs were cultured in Luria-Bertani medium supplemented with the appropriate antibiotics at 28°C for 36 h, and then harvested and re-suspended in infiltration buffer [10 mM 2-(N-morpholine)-ethane sulfonic acid (MES), 10 mM $MgCl_2$ (pH 5.6), and 200 μM acetosyringone] to the appropriate concentration. Infiltrations were performed at a final OD_{600} of 0.4-0.6 (Meng et al. 2015). After incubation for 1 h at room temperature, the *A. tumefaciens* suspensions were infiltrated into plant leaves using needleless syringes.

Total RNA extraction and qRT-PCR analysis

Total RNA was extracted from the whole leaves before and after inoculation using TRIzol reagent (Invitrogen, Carlsbad, CA, USA). RNA concentration was quantitated, and 1 μg total RNA was used as template for reverse transcription into cDNA with a PrimeScript RT Reagent Kit with gDNA Eraser (TaKaRa, China) according to the product manuals. qRT-PCR was performed using SYBR Green mix (CWBio, Beijing, China) on an iQ7 Real-Time Cycler (Life Technologies, USA). For qRT-PCR analysis, the cDNA was diluted 10 times, and 2 μl reaction products were used as template in a reaction under the following conditions: 95°C for 10 min, and 40 cycles of 95°C for 15 s and 60°C for 30 s. The fold changes in target gene expression were normalized using *N. benthamiana* and *N. tabacum ACTIN* as the internal control. Primers used for qRT-PCR are listed in Table S1. Three biological replicates were included in the assays.

MAPK activation assay

To detect the phosphorylation of MAPKs (Zhang and Klessig 2001; Schwessinger et al. 2011), 6-week-old soil-grown *N. benthaminana* leaves were infiltrated with water containing 10 μM peptides. Proteins were extracted with glycerol-Tris-EDTA-NaCl (GTEN) buffer (25 mM Tris–HCl (pH 7.5), 15 mM $MgCl_2$, 15 mM EGTA, 75 mM NaCl, 1 mM DTT, 0.1% NP-40, 5 mM p-nitrophenylphosphate, 60 mM β-glycerophosphate, 0.1 mM Na_3VO_3, 1 mM NaF, 1 mM PMSF, 5 μg/mL leupeptin, and 5 μg/mL aprotinin), and then centrifuged at 12,000 *g* for 15 min at 4 °C. The protein concentration of the supernatant was measured using the Super-Bradford Protein Assay Kit (CWBIO, CW0013S). Protein (20 μl per sample) was separated on a 15% acrylamide gel using sodium dodecyl sulfate polyacrylamide gel electrophoresis (SDS-PAGE)

and transferred onto a PVDF membrane for immunoblotting with anti-phospho-p44/42 MAPK (Erk1/2) (Thr202/Tyr204) (D13.14.4E) XP rabbit mAb antibody (Cell Signaling Technology). The large subunit of ribulose-1,5-bisphosphate carboxylase/oxygenase (Rubisco) was visualized by Ponceau staining of the PVDF membrane. Three biological replicates were included in the assays.

Callose staining

N. benthamiana leaves were collected at 24 hours post injection with water, or 10 μM of either NbPPI1, flg22, or PIP1, and then immediately immersed in 100 % ethanol. To remove the background fluorescence, the samples were stained with solution A (acetic acid: ethanol, 1:3) for 2 h, and then rinsed twice with 150 mM phosphate buffer (pH 8.0). Callose was stained with aniline blue solution [0.02 % aniline blue, 150 mM K_2HPO_4 (pH 8.0)] for 4 h in the dark. Aniline blue-stained leaves were mounted in 30 % glycerol and observed using an Olympus BX-51TRF fluorescence microscope (Olympus, Tokyo, Japan). The number of callose loci was quantified using ImageJ.

VIGS assay

A. tumefaciens strain GV3101 carrying different *pTRV2* constructs were mixed with *TRV1* in equal ratios to a final OD_{600} of 0.25, and *pTRV2:PDS* was used to visualize the silencing process. The lower leaves of two-leaf-stage *N. benthamiana* plants were infiltrated as described previously (Liu et al. 2002), and the upper leaves of VIGS plants were used to analyze the efficiency of gene silencing by qRT-PCR. The VIGS primers used in this study are shown in Table S1.

Oxidative burst test

A luminol-based assay was used to quantify ROS production in treated leaves. Leaf discs were cut from 6-week-old plants using a 5-mm hole puncher, placed into a well of a white 96-well plate containing water, and kept in the dark overnight. The water was replaced with 200 μl master mix containing 30 μg/mL luminol, 20 μg/mL horseradish peroxidase, and 1 μg peptide under dark condition. Luminescence was measured at 535 nm (excitation 490 nm) directly after peptide addition in a TECAN Infinite F200 microplate reader (TECAN, Switzerland) at 1-min intervals over 40 min.

ACKNOWLEDGEMENTS

We would like to thank Professor Jun Liu (Institute of Microbiology，Chinese Academy of Sciences) for helpful suggestions on the manuscript, and Northwest A&F University Life Science Research Core Services for providing advanced facility. This work was supported by the National Natural Science Foundation of China (31125022 and 31930094), the China Agriculture Research System (CARS-09), and the Programme of Introducing Talents of Innovative Discipline to Universities (Project 111) from the State Administration of Foreign Experts Affairs (#B18042).

AUTHOR CONTRIBUTIONS

W.S. and Q.W. designed the experiments, Q.W., M.S. and X.K. performed the experiments, Y.Y., Q.Z., G.H., W.L. and Y.M. contributed materials, Q.W., Y.M., and W. S. wrote the manuscript with contributions from all authors. All authors read and approved of the article.

REFERENCES

Asai T, Tena G, Plotnikova J, Willmann MR, Chiu WL, Gomez-Gomez L, Boller T, Ausubel FM, Sheen J (2002) MAP kinase signalling cascade in *Arabidopsis* innate immunity. **Nature** 415: 977–983

Benedetti M, Verrascina I, Pontiggia D, Locci F, Mattei B, De Lorenzo G, Cervone F (2018) Four *Arabidopsis* berberine bridge enzyme-like proteins are specific oxidases that inactivate the elicitor-active oligogalacturonides. **Plant J** 94: 260–273

Boller T, Felix G (2009) A renaissance of elicitors: Perception of microbe-associated molecular patterns and danger signals by pattern-recognition receptors. **Ann Rev Plant Biol** 60: 379–406

Cederholm HM, Benfey PN (2015) Distinct sensitivities to phosphate deprivation suggest that RGF peptides play disparate roles in *Arabidopsis thaliana* root development. **New Phytol** 207: 683–691.

Cervone F, De Lorenzo G, Degrà L, Salvi G (1987) Elicitation of necrosis in *Vigna unguiculata* Walp. by homogeneous *Aspergillus niger* endo-polygalacturonase and by alpha-d-galacturonate oligomers. **Plant Physiol** 85: 626–630

Chaparro-Garcia A, Wilkinson RC, Gimenez-Ibanez S, Findlay K, Coffey MD, Zipfel C, Rathjen JP, Kamoun S, Schornack S (2011) The receptor-like kinase SERK3/BAK1 is required for basal resistance against the late blight pathogen *Phytophthora infestans* in *Nicotiana benthamiana*. **PLoS ONE** 6: e10068

Chen YL, Fan KT, Hung SC, Chen YR (2020) The role of peptides cleaved from protein precursors in eliciting plant stress reactions. **New Phytol** 225: 2267-2282

Chinchilla D, Zipfel C, Robatzek S, Kemmerling B, Nurnberger T, Jones JDG, Felix G, Boller T (2007) A flagellin-induced complex of the receptor FLS2 and BAK1 initiates plant defence. **Nature** 448: 497–501

Choi HW, Manohar M, Manosalva P, Tian M, Moreau M, Klessig DF (2016) Activation of plant innate immunity by extracellular high mobility group box 3 and its inhibition by salicylic acid. **PLoS Pathog** 12: e1005518

Coll NS, Epple P, Dangl JL (2011) Programmed cell death in the plant immune system. **Cell Death Differ** 18: 1247–1256

Curtis MD, Grossniklaus U (2003) A gateway cloning vector set for high-throughput functional analysis of genes in planta. **Plant Physiol** 133: 462–469

De Lorenzo G, Ferrari S, Cervone F, Okun E (2018) Extracellular DAMPs in plants and mammals: Immunity, tissue damage and repair. **Trends Immunol** 39: 937–950

Denoux C, Galletti R, Mammarella N, Gopalan S, Werck D, De Lorenzo G, Ferrari S, Ausubel FM, Dewdney J (2008) Activation of defense response pathways by OGs and Flg22 elicitors in *Arabidopsis* seedlings. **Mol Plant** 1: 423–445

Evangelisti E, Gogleva A, Hainaux T, Doumane M, Tulin F, Quan C, Yunusov T, Floch K, Schornack S (2017) Time-resolved dual transcriptomics reveal early

induced *Nicotiana benthamiana* root genes and conserved infection-promoting *Phytophthora palmivora* effectors. **BMC Biol** 15: 39

Fan GJ, Yang Y, Li TT, Lu WQ, Du Y, Qiang XY, Wen QJ, Shan WX (2018) A *Phytophthora capsici* RXLR effector targets and inhibits a plant PPIase to suppress endoplasmic reticulum-mediated immunity. **Mol Plant** 11: 1067–1083

Fernandez-Pozo N, Rosli HG, Martin GB, Mueller LA (2015) The SGN VIGS Tool: User-Friendly software to design Virus-Induced Gene Silencing (VIGS) constructs for functional genomics. **Mol Plant** 8: 486–488

Galletti R, Ferrari S, De Lorenzo G (2011) *Arabidopsis* MPK3 and MPK6 play different roles in basal and oligogalacturonide-or flagellin-induced resistance against *Botrytis cinerea*. **Plant Physiol** 157: 804–814

Gehl C, Waadt R, Kudla J, Mendel RR, Hansch R (2009) New GATEWAY vectors for high throughput analyses of protein-protein interactions by Bimolecular Fluorescence Complementation. **Mol Plant** 2: 1051–1058

Ghorbani S, Lin YC, Parizot B, Fernandez A, Njo MF, Van de Peer Y, Beeckman T, Hilson P (2015) Expanding the repertoire of secretory peptides controlling root development with comparative genome analysis and functional assays. **J Exp Bot** 66: 5257–5269

Gully K, Pelletier S, Guillou MC, Ferrand M, Aligon S, Pokotylo I, Perrin A, Vergne E, Fagard M, Ruelland E, Grappin P, Bucher E, Renou JP, Aubourg S (2019) The SCOOP12 peptide regulates defense response and root elongation in *Arabidopsis thaliana*. **J Exp Bot** 70: 1349–1365

Gust AA, Pruitt R, Nurnberger T (2017) Sensing danger: Key to activating plant immunity. **Trends Plant Sci** 22: 779–791

Hander T, Fernandez-Fernandez AD, Kumpf RP, Willems P, Schatowitz H, Rombaut D, Staes A, Nolf J, Pottie R, Yao PF, Goncalves A, Pavie B, Boller T, Gevaert K, Van Breusegem F, Bartels S, Stael S (2019) Damage on plants activates Ca^{2+}-dependent metacaspases for release of immunomodulatory peptides. **Science** 363: eaar7486

Heese A, Hann DR, Gimenez-Ibanez S, Jones AME, He K, Li J, Schroeder JI, Peck SC, Rathjen JP (2007) The receptor-like kinase SERK3/BAK1 is a central regulator of innate immunity in plants. **Proc Natl Acad Sci USA** 104: 12217–12222

Heil M, Ibarra-Laclette E, Adame-Alvarez RM, Martinez O, Ramirez-Chavez E, Molina-Torres J, Herrera-Estrella L (2012) How plants sense wounds: Damaged-self recognition is based on plant-derived elicitors and induces Octadecanoid signaling. **PLoS ONE** 7: e30537

Heil M, Land WG (2014) Danger signals-damaged-self recognition across the tree of life. **Front Plant Sci** 5: 578

Hou SG, Liu ZY, Shen HX, Wu DJ (2019) Damage-associated molecular pattern-triggered immunity in plants. **Front Plant Sci** 10: 646

Hou SG, Wang X, Chen DH, Yang X, Wang M, Turra D, Di Pietro A, Zhang W (2014) The secreted peptide PIP1 amplifies immunity through Receptor-Like Kinase 7. **PLoS Pathog** 10: e1004331

Hu Z, Zhang H, Shi K (2018) Plant peptides in plant defense responses. **Plant Signal Behav** 13: e1475175.

Huffaker A, Dafoe NJ, Schmelz EA (2011) ZmPep1, an ortholog of *Arabidopsis* elicitor peptide 1, regulates maize innate immunity and enhances disease resistance. **Plant Physiol** 155: 1325–1338

Huffaker A, Pearce G, Ryan CA (2006) An endogenous peptide signal in *Arabidopsis* activates components of the innate immune response. **Proc Natl Acad Sci USA** 103: 10098–10103

Kaeothip S, Ishiwata A, Ito Y (2013) Stereoselective synthesis of *Arabidopsis* CLAVATA3 (CLV3) glycopeptide, unique protein post-translational modifications of secreted peptide hormone in plant. **Org Biomol Chem** 11: 5892–5907

Krol E, Mentzel T, Chinchilla D, Boller T, Felix G, Kemmerling B, Postel S, Arents M, Jeworutzki E, Al-Rasheid KAS, Becker D, Hedrich R (2010) Perception of the *Arabidopsis* danger signal peptide 1 Involves the pattern recognition receptor AtPEPR1 and its close homologue AtPEPR2. **J Biol Chem** 285: 13471–13479

Li L, Li CY, Lee GI, Howe GA (2002) Distinct roles for jasmonate synthesis and action in the systemic wound response of tomato. **Proc Natl Acad Sci USA** 99: 6416–6421

Liu YL, Schiff M, Dinesh-Kumar SP (2002) Virus-induced gene silencing in tomato. **Plant J** 31: 777–786

Matos JL, Fiori CS, Silva-Filho MC, Moura DS (2008) A conserved dibasic site is essential for correct processing of the peptide hormone AtRALF1 in *Arabidopsis thaliana*. **FEBS Lett** 582: 3343–3347

Matsubayashi Y (2011) Post-translational modifications in secreted peptide hormones in plants. **Plant Cell Physiol** 52: 5–13

Matsubayashi Y, Sakagami Y (1996) Phytosulfokine, sulfated peptides that induce the proliferation of single mesophyll cells of *Asparagus officinalis* L. **Proc Natl Acad Sci USA** 93: 7623–7627

Meng YL, Huang YH, Wang QH, Wen QJ, Jia JB, Zhang Q, Huang GY, Quan JL, Shan WX (2015) Phenotypic and genetic characterization of resistance in *Arabidopsis thaliana* to the oomycete pathogen *Phytophthora parasitica*. **Front Plant Sci** 6: 378

Mosher S, Seybold H, Rodriguez P, Stahl M, Davies KA, Dayaratne S, Morillo SA, Wierzba M, Favery B, Keller H, Tax FE, Kemmerling B (2013) The tyrosine-sulfated peptide receptors PSKR1 and PSY1R modify the immunity of *Arabidopsis* to biotrophic and necrotrophic pathogens in an antagonistic manner. **Plant J** 73: 469–482

Mueller K, Bittel P, Chinchilla D, Jehle AK, Albert M, Boller T, Felix G (2012) Chimeric FLS2 receptors reveal the basis for differential flagellin perception in *Arabidopsis* and tomato. **Plant Cell** 24: 2213–2224

Najafi J, Brembu T, Vie AK, Viste R, Winge P, Somssich IE, Bones AM (2020) PAMP-INDUCED SECRETED PEPTIDE 3 modulates immunity in *Arabidopsis*. **J Exp Bot** 71: 850–864

Oelkers K, Goffard N, Weiller GF, Gresshoff PM, Mathesius U, Frickey T (2008) Bioinformatic analysis of the CLE signaling peptide family. **BMC Plant Biol** 8: 1

Ohyama K, Ogawa M, Matsubayashi Y (2008) Identification of a biologically active, small, secreted peptide in *Arabidopsis* by in silico gene screening, followed by LC-MS-based structure analysis. **Plant J** 55: 152–160

Ökmen B, Bachmann D, de Wit P (2019) A conserved GH17 glycosyl hydrolase from plant pathogenic Dothideomycetes releases a DAMP causing cell death in tomato. **Mol Plant** 20: 1710–1721

Olsson V, Joos L, Zhu S, Gevaert K, Butenko MA, De Smet I (2019) Look closely, the beautiful may be small: Precursor-derived peptides in plants. **Annu Rev Plant Biol** 70: 153–186

Pearce G, Strydom D, Johnson S, Ryan CA (1991) A polypeptide from tomato leaves induces wound-inducible proteinase inhibitor proteins. **Science** 253: 895–897

Perraki A, DeFalco TA, Derbyshire P, Avila J, Sere D, Sklenar J, Qi XY, Stransfeld L, Schwessinger B, Kadota Y, Macho AP, Jiang SS, Couto D, Torii KU, Menke FLH, Zipfel C (2018) Phosphocode-dependent functional dichotomy of a common co-receptor in plant signalling. **Nature** 561: 248–252

Postel S, Kufner I, Beuter C, Mazzotta S, Schwedt A, Borlotti A, Halter T, Kemmerling B, Nurnberger T (2010) The multifunctional leucine-rich repeat receptor kinase BAK1 is implicated in *Arabidopsis* development and immunity. **Eur J Cell Biol** 89: 169–174

Sandhu D, Tasma IM, Frasch R, Bhattacharyya MK (2009) Systemic acquired resistance in soybean is regulated by two proteins, orthologous to *Arabidopsis* NPR1. **BMC Plant Biol** 9: 105

Sauter M (2015) Phytosulfokine peptide signalling. **J Exp Bot** 66: 5160–5168

Schulze B, Mentzel T, Jehle AK, Mueller K, Beeler S, Boller T, Felix G, Chinchilla D (2010) Rapid heteromerization and phosphorylation of ligand-activated plant transmembrane receptors and their associated kinase BAK1. **J Biol Chem** 285: 9444–9451

Schwessinger B, Roux M, Kadota Y, Ntoukakis V, Sklenar J, Jones A, Zipfel C (2011) Phosphorylation-dependent differential regulation of plant growth, cell death, and innate immunity by the regulatory receptor-like kinase BAK1. **PLoS Genet** 7: e1002046

Segonzac C, Monaghan J (2019) Modulation of plant innate immune signaling by small peptides. **Curr Opin Plant Biol** 51: 22–28

Shiu SH, Bleecker AB (2001) Receptor-like kinases from *Arabidopsis* form a monophyletic gene family related to animal receptor kinases. **Proc Natl Acad Sci USA** 98: 10763-10768

Srivastava R, Liu JX, Guo HQ, Yin YH, Howell SH (2009) Regulation and processing of a plant peptide hormone, AtRALF23, in *Arabidopsis*. **Plant J** 59: 930–939

Stegmann M, Monaghan J, Smakowska-Luzan E, Rovenich H, Lehner A, Holton N, Belkhadir Y, Zipfel C (2017) The receptor kinase FER is a RALF-regulated scaffold controlling plant immune signaling. **Science** 355: 287–289

Sun JQ, Jiang HL, Li CY (2011) Systemin/Jasmonate-mediated systemic defense signaling in tomato. **Mol Plant** 4: 607–615

Sun YD, Li L, Macho AP, Han ZF, Hu ZH, Zipfel C, Zhou JM, Chai JJ (2013) Structural basis for flg22-Induced activation of the *Arabidopsis* FLS2-BAK1 immune complex. **Science** 342: 624–628

Tavormina P, De Coninck B, Nikonorova N, De Smet I, Cammue BP (2015) The Plant Peptidome: An expanding repertoire of structural features and biological functions. **Plant Cell** 27: 2095–2118

Vie AK, Najafi J, Liu B, Winge P, Butenko MA, Hornslien KS, Kumpf R, Aalen RB, Bones AM, Brembu T (2015) The IDA/IDA-LIKE and PIP/PIP-LIKE gene families in *Arabidopsis*: Phylogenetic relationship, expression patterns, and transcriptional effect of the PIPL3 peptide. **J Exp Bot** 66: 5351–5365

Wang W, Feng B, Zhou JM, Tang D (2020) Plant immune signaling: Advancing on two frontiers. **J Integr Plant Biol**, 62:2–24

Wang XD, Boevink P, McLellan H, Armstrong M, Bukharova T, Qin ZW, Birch PRJ (2015) A host KH RNA-binding protein is a susceptibility factor targeted by an RXLR effector to promote Late Blight disease. **Mol Plant** 8: 1385–1395

Wang X, Hou SG, Wu QQ, Lin MY, Acharya BR, Wu DJ, Zhang W (2017) IDL6-HAE/HSL2 impacts pectin degradation and resistance to *Pseudomonas syringae* pv tomato DC3000 in *Arabidopsis* leaves. **Plant J** 89: 250–263

Wang Y, Wang YC, Wang YM (2020) Apoplastic proteases - powerful weapons against pathogen infection in plants. **Plant Commun** 1:10085

Wu Y, Zhou JM (2013) Receptor-like kinases in plant innate immunity. **J Integr Plant Biol**, 55:1271–1286.

Yamada K, Yamashita-Yamada M, Hirase T, Fujiwara T, Tsuda K, Hiruma K, Saijo Y (2016) Danger peptide receptor signaling in plants ensures basal immunity upon pathogen-induced depletion of BAK1. **EMOB J** 35: 46–61

Zhang H, Hu ZJ, Lei C, Zheng CF, Wang J, Shao SJ, Li X, Xia XJ, Cai XZ, Zhou J, Zhou YH, Yu JQ, Foyer CH, Shi K (2018) A plant phytosulfokine peptide initiates auxin-dependent immunity through cytosolic Ca^{2+} signaling in tomato. **Plant Cell** 30: 652–667

Zhang SQ, Klessig DF (2001) MAPK cascades in plant defense signaling. **Trends Plant Sci** 6: 520–527

Zipfel C (2014) Plant pattern-recognition receptors. **Trends Immunol** 35: 345–351

Figures

Figure 1. Identification of NbPROPPI1 and NbPROPPI2

(**A**) Schematic representation of PROPPI and sequence alignment of NtPROPPI homologs in *N. benthamiana*. (**B**) Subcellular localization of NbPROPPI1. (**C**) Subcellular localization of NbPROPPI2. The assay was performed by transient expression of NbPROPPI1/2-GFP and a mCherry-tagged plasma membrane marker in *N. benthamiana* leaf epidermal cells. The white dotted square marks the cell membrane. All scale bars indicate 20 μm.

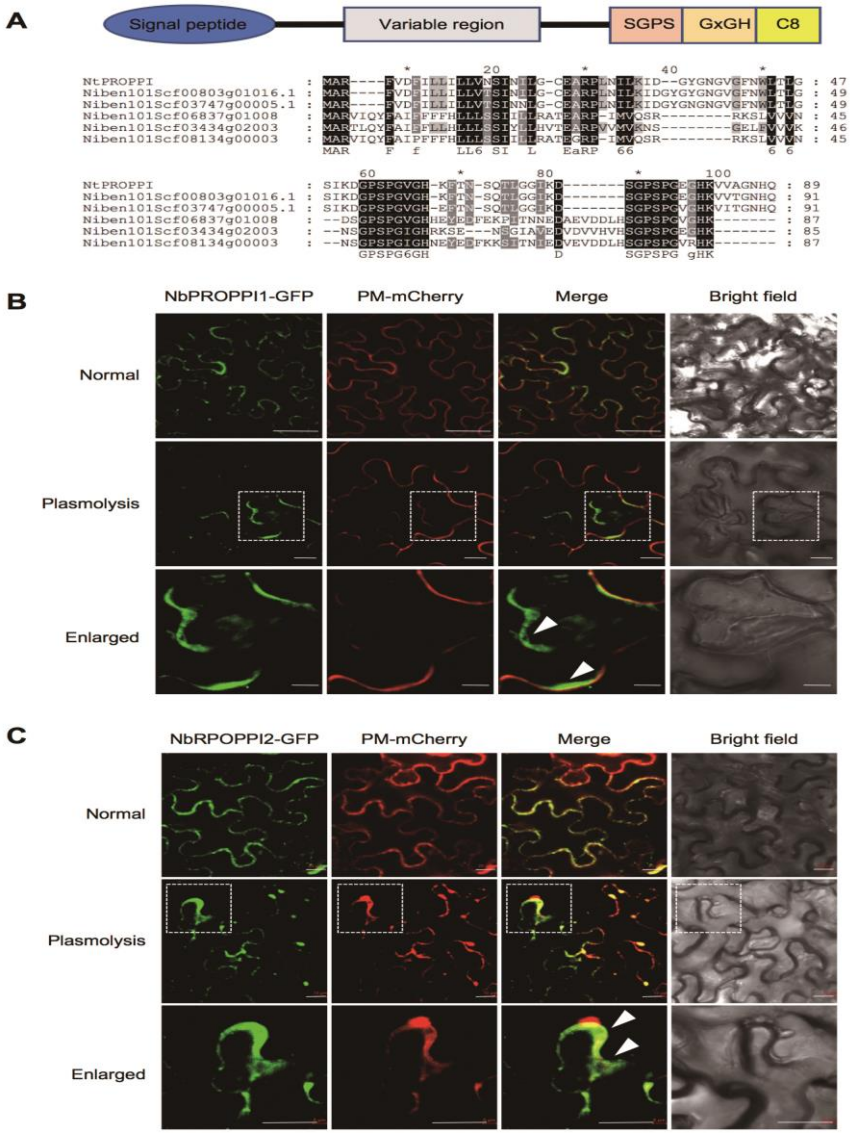

Figure 2. *NbPROPPI* provokes the plant immune response in *N. tabacum*.

(**A**) *NbPROPPI1* and *NbPROPPI2* induced chlorosis in the leaves of *N. tabacum* cultivars YunYan85, QinYan95, and HD. *Agrobacterium tumefaciens* GV3101 cells carrying *NbPROPPI1* and *NbPROPPI2* with an OD_{600} value of 0.4 were infiltrated into the 6-week-old leaves of *N. benthamiana*, *N. tabacum* cultivars YunYan85, QinYan95, HD, and K346, potato (differential line R5), and tomato cultivar Alisa Craig. Photographs were taken at 5 dpi for *N. tabacum* and *N. benthamiana*, and at 7 dpi for potato and tomato. (**B**) *N. tabacum* leaves infiltrated with *A. tumefaciens* GV3101 harboring *NbPROPPI1* or *GUS* constructs were challenged by *P. parasitica*. Photographs were taken at 48 h post-inoculation (hpi). (**C**) Mean lesion diameters of the inoculated leaves. (**D**) *P. parasitica* colonization was determined by qPCR. Total genomic DNA from *P. parasitica*-infected regions was isolated at 48 hpi. Primers specific for *N. tabacum ACTIN* and the *P. parasitica UBC* were used to determine *P. parasitica* biomass in infected plant tissues. Error bars indicate SD and asterisks indicate significant differences determined based on Student's *t*-test ($^{***}P < 0.001$, $^{**}P < 0.01$). Similar results were obtained from at least three individual experiments.

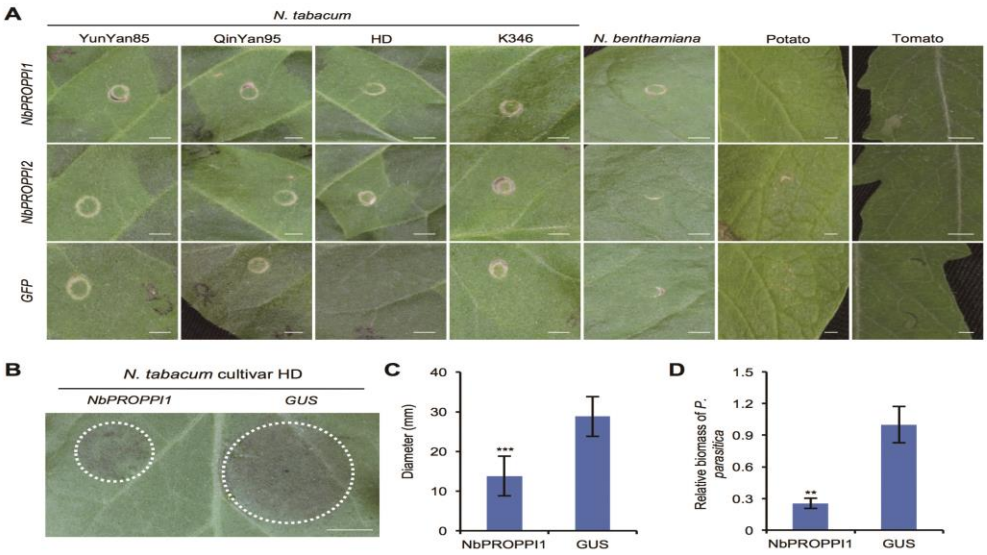

Figure 3. Expression of *NbPROPPI1* and *NbPROPPI2*

(**A**) The expression of *NbPROPPI1* and *NbPROPPI2* at different stages of infection was determined by qRT-PCR. The 6-week-old leaves from *N. benthamiana* were inoculated with *P. parasitica*. Total RNA was extracted from infected leaves at 0, 3, 6, 12, 24, and 36 hpi. (**B-D**) qRT-PCR analysis for the expression of *NbPROPPI1* and *NbPROPPI2* in *N. benthamiana* at different time points following exposure to MeSA, ACC, and MeJA. Total RNA was extracted from infected leaves at 0, 3, and 6 hpi. *N. benthamiana ACTIN* was used for normalization. Error bars indicate SD and asterisks indicate significant differences determined based on Student's *t*-test ($^{***}P < 0.001$, $^{**}P < 0.01$). Similar results were obtained from at least three individual experiments.

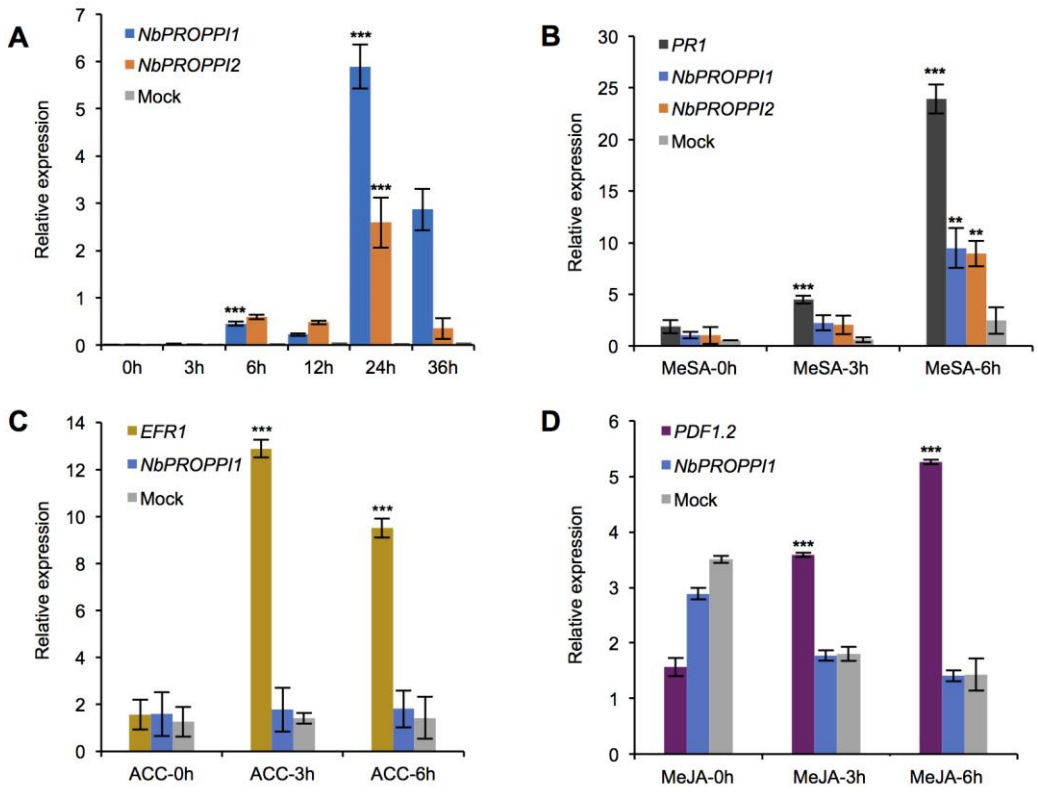

Figure 4. NbPPI treatment enhances plant resistance to *Phytophthora* pathogens.

Colonization of *P. parasitica* (**A**) and *P. infestans* (**B**) in *N. benthamiana* leaves after treatment with NbPPI. The 6-week-old *N. benthamiana* leaves were infiltrated with 1 μM NbPPI1 or 1 μM NbPPI2, and 24 h later the leaves were detached and inoculated with *P. parasitica* or *P. infestans*. Photographs were taken at 2 dpi for *P. infestans* and 5 dpi for *P. parasitica*. The mean lesion diameters are shown, and the relative biomass of *Phytophthora* was determined by qPCR with primers specific for the *N. benthamiana ACTIN* and the *Phytophthora UBC*. Error bars represent SD and asterisks indicate significant differences based on Student's *t*-test ($^{***}P < 0.001$, $^{**}P < 0.01$). Similar results were obtained from at least three individual experiments.

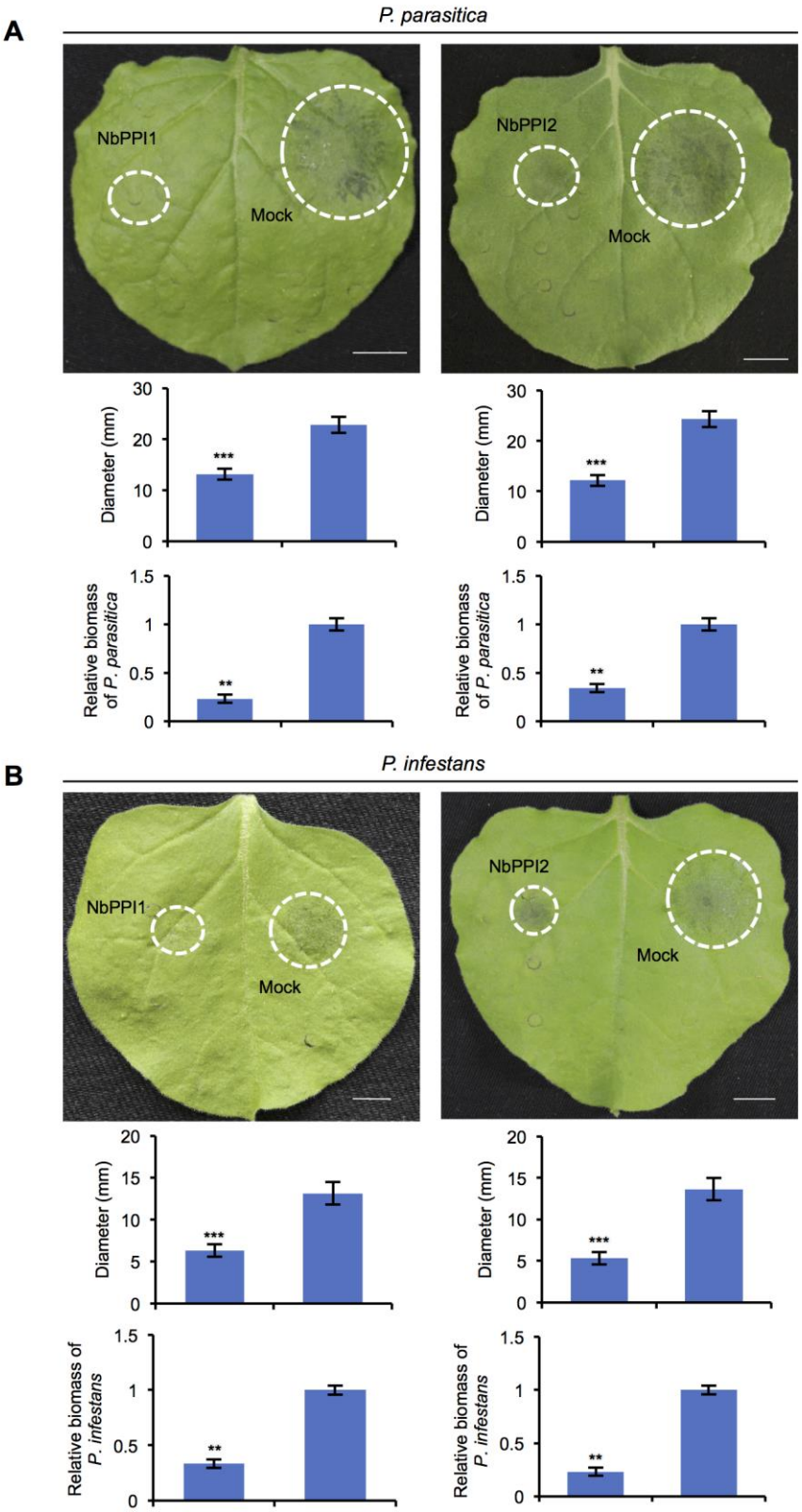

Figure 5. NbPPI1 activates immune responses in *N. benthamiana*.

(**A-B**) The expression of immune genes *WRKY33* and *FRK* in 6-week-old *N. benthamiana* leaves 6 h post treatment with 1 μM NbPPI. (**C**) MAPK activation induced by NbPPI1 in 6-week-old *N. benthamiana* leaves exposed to 10 μM NbPPI1 at 10 min and 15 min. Total protein was extracted and analyzed by immunoblotting using antibodies against phospho-p44/42 MAPK and actin. (**D**) Quantification of ROS production in *N. benthamiana* leaf discs treated with 1 μM of each peptide. Total relative luminescent units (RLUs) were detected over 30 min using leaf discs of the 6-week-old *N. benthamiana* leaves. Graphs display averages of 12 replicates. (**E**) Fluorescence microscopy imaging of callose deposition. The leaves were stained with aniline blue 4 h after infiltration with 1 μM of each peptide. All scale bars indicate 200 μm. (**F**) Quantification of callose deposition. Error bars indicate SD and asterisks indicate significant differences determined based on Student's *t*-test ($^{***}P < 0.001$, $^{**}P < 0.01$). Similar results were obtained from at least three individual experiments.

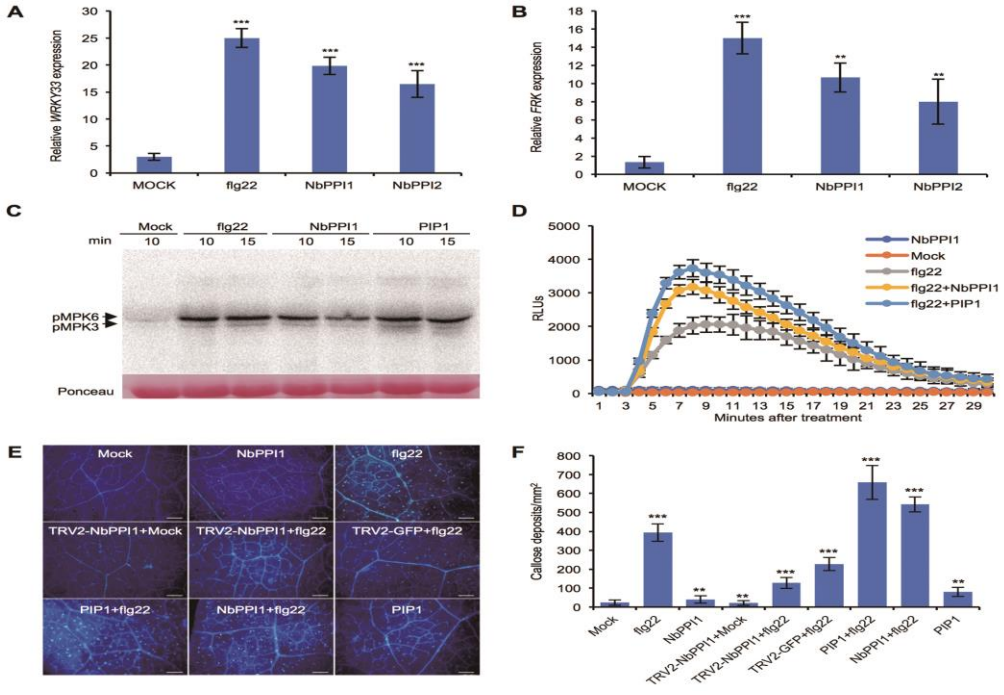

Figure 6. *NbPROPPI*-silenced *N. benthamiana* plants showed increased susceptibility to *P. parasitica*

(**A**) *P. parasitica* colonization in *TRV2-NbPROPPI*- or *TRV2-GFP*-infiltrated leaves. Photographs were taken at 48 hpi. (**B**) The mean lesion diameters of the *P. parasitica*- inoculated leaves. (**C**) *P. parasitica* colonization was determined by qPCR. Total genomic DNA from *P. parasitica*-infected leaves at 48 hpi was extracted and *P. parasitica* biomass was quantitated by qPCR. (**D**) The silencing efficiencies of *NbPROPPI1* and *NbPROPPI2* were determined by qRT-PCR using cDNA synthesized from total RNA extracted from *TRV2-NbPROPPI*- and *TRV2-GFP*-infiltrated plants. Error bars indicate SD and asterisks indicate significant differences determined based on Student's *t*-test ($^{**}P < 0.01$). Similar results were obtained from at least three individual experiments.

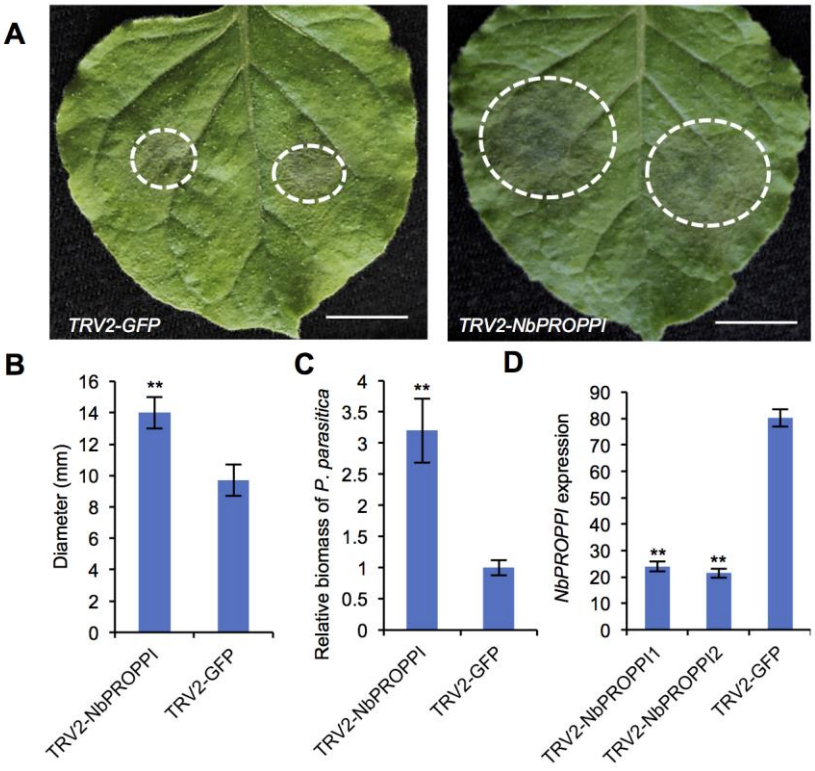

Figure 7. The distinct 8 amino acid region at the C-terminus of NbPPl1 is essential for its immunity activity

(**A**) The 6-week-old *N. benthamiana* leaves were infiltrated with 1 μM NbPPI1, NbPPI1-ΔC8 or mock (H_2O) followed by inoculation with *P. parasitica* and were scored for the mean lesion diameters and relative biomass of *P. parasitica*. Photographs were taken at 48 hpi. (**B**) Suppressed growth of *N. benthamiana* roots treated with 1 μM NbPPI1 and 1 μM NbPPI1-ΔC8 for 25 days. (**C**) Quantitation of ROS production in *N. benthamiana* leaf discs pretreated with 1 μM of each peptide. Total RLUs were detected over 30 min using leaf discs of the 6-week-old plants. Graphs display averages of 12 replicates. Error bars represent SD and asterisks indicate significant differences based on Student's *t*-test ($^{**}P < 0.01$). Similar results were obtained from at least three individual experiments.

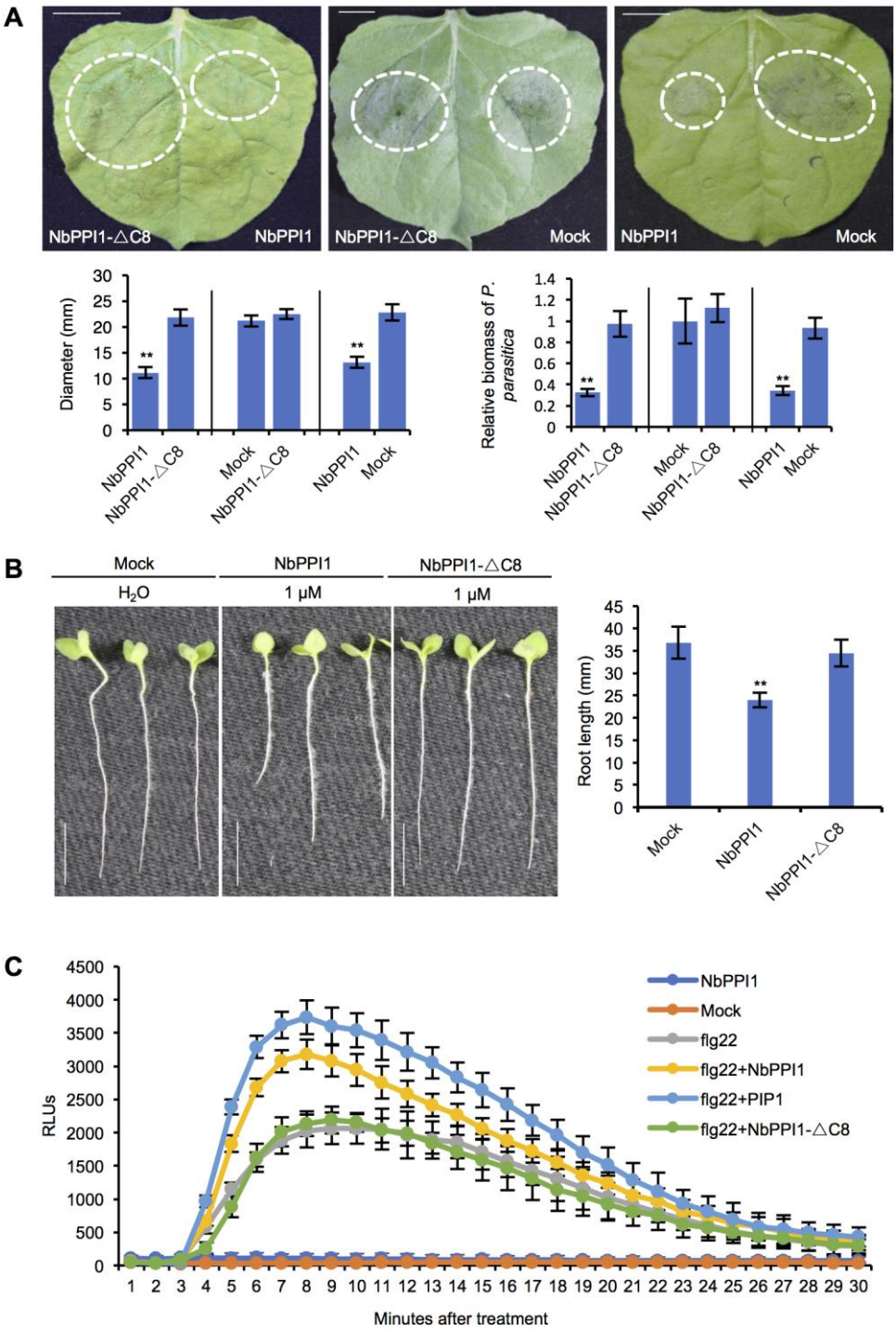

Figure 8. *NbPROPPI1*-activated plant immunity is *BAK1*-dependent in *N. benthamiana*

(**A**) *P. parasitica* colonization in *TRV2-BAK1*- or *TRV2-GFP*-infiltrated leaves pretreated with 10 μM NbPPI1. Photographs were taken at 48 hpi. The mean lesion diameters and relative biomass of *P. parasitica* are shown. **(B)** The quantitation of ROS production in *TRV2-BAK1* or *TRV2-GFP*-infiltrated leaves after treatment with 1 μM peptides. (**C**) The relative expression of the defense-related gene *WRKY33* in *TRV2-BAK1*-infiltrated leaves at different stages of *P. parasitica* infection. (D) The silencing efficiencies of *BAK1* were determined by qRT-PCR. Error bars represent SD and asterisks indicate significant differences based on Student's *t*-test ($^{***}P<0.001$, $^{**}P < 0.01$). Similar results were obtained from at least three individual experiments.